EURASIP Journal on Wireless Communications and Networking
a SpringerOpen Journal

RESEARCH Open Access

An approach to the modulation recognition of MIMO radar signals

Xiaojing Wang*, Ying Xiong, Bin Tang and Yunhao Li

Abstract

Multiple-input multiple-output (MIMO) radar is a new radar system and draws more and more attentions in recent years. Along with the development of MIMO radar, the MIMO radar countermeasure is brought into being. Since the modulation recognition is of great significance in the electronic reconnaissance, this article presents a modulation recognition method for the signals of the emerging MIMO radar. Signals of interest are classified into three categories based on instantaneous autocorrelation spectrum analysis first. Then non-coding MIMO radar signals are discriminated by spectrum analysis, and coding MIMO radar signals are recognized by source number estimation algorithm. Meanwhile, the sub-carrier numbers of some kinds of MIMO radar signals are estimated. Simulation results verify the effectiveness of the method and the overall correct recognition rate is over 90% when the value of SNR is above 0 dB.

Keyword: Modulation recognition, MIMO radar signal, Instantaneous autocorrelation spectrum, Source number estimation, Sub-carrier number

1. Introduction

The concept of multiple-input multiple-output (MIMO) radar, which comes from communication system, has drawn considerable attention in recent years from both researchers and practitioners [1]. It builds a bridge between the research of radar and communication. MIMO radar is generally divided into two categories, one is statistical MIMO radar with widely separated antennas, and the other is coherent MIMO radar with co-located antennas. In both categories of MIMO radar system, multiple transmit antennas are employed to emit specific waveforms and multiple receive antennas process the reflected signals jointly. MIMO radar offers quite a lot of advantages, such as more degrees of freedom, higher resolution, and sensitivity and better parameter identifiability [2-4]. These advantages mostly result from waveform diversity. Due to the waveform diversity, intercepted signals in reconnaissance receiver are multi-carrier signals. Accordingly, signal detection, parameter estimation, and modulation recognition are vastly different from single-carrier (SC) signals adopted by conventional radars. As a result, it poses an emerging and powerful challenge in electronic countermeasures.

In order to occupy an advantageous position in the future electronic warfare, we need to investigate the feature of MIMO radar and study its electronic countermeasures. This article discusses the modulation recognition of MIMO radar signals, which is of great significant in the electronic reconnaissance. Since there are some actual difficulties in engineering practice for statistical MIMO radar, hereinafter we focus on coherent MIMO radar.

The reconnaissance technology of MIMO radar is rarely studied in the published literatures. Liang [5] and Xing et al. [6] discussed about the electronic reconnaissance technology of MIMO radar at system design and conceptual angle. Tang et al. [7] provided a new reconnaissance technology for MIMO radar. The aim of the article is to discriminate whether it is MIMO radar by the number of orthogonal waveforms. However, the location of suspicious radar is as known information, which is usually unknown in actual environment. Besides, Chen et al. [8] and Hassan et al. [9] were about the modulation identification of MIMO system, which is adopted in the wireless communication field. In [8], the combination of second- and fourth-order of cumulants was used as the feature parameters, which were utilized to discriminate the orthogonal frequency division multiplexing signals from the SC modulations. In [9], high-order statistics and neural networks were

* Correspondence: wangadlinna@yahoo.com.cn
School of Electronic Engineering, University of Electronic Science and Technology of China, Chengdu, People's Republic of China

employed to identify the modulation type of MIMO system with and without channel state information.

Based on the instantaneous autocorrelation spectrum of received signals, an approach to the modulation recognition of MIMO radar signals is proposed in this article. For conventional radar, SC signal is often adopted, such as monopulse (MP) signal, linear frequency modulation (LFM) signal, phase-coded (PC) signal, and frequency-coded (FC) signal. For MIMO radar, four basic modulation types [10-12] are involved in this article: MP-MIMO (orthogonal MP signal in MIMO radar), LFM-MIMO (orthogonal LFM signal in MIMO radar), PC-MIMO (orthogonal PC signal in MIMO radar), and FC-MIMO (orthogonal FC signal in MIMO radar). Here, we need to discriminate MIMO radar signal from conventional radar signal and recognize the modulation type of MIMO radar signal.

The remainder of this article is organized as follows. In Section 2, four basic emitting signal models of MIMO radar are given. The recognition method is introduced in Section 3. Instantaneous autocorrelation spectrum analysis, frequency spectrum analysis, and source number estimation algorithm (SNEA) are involved in this section. Simulation results are given in Section 4 and conclusions are drawn in Section 5.

2. Signal models

Assuming that the transmitting arrays of MIMO radar are uniform linear arrays (ULA), in the reconnaissance receiver, the four basic received MIMO signal models can be expressed as follows [10-12].

$$s_{\mathrm{MP-MIMO}}[n] = \sum_{m=1}^{M} \exp\{j2\pi[f_0 + (m-1)f_p] t + j(m-1)\Delta\phi\}|_{t=nT_s} \tag{1}$$

$$s_{\mathrm{LFM-MIMO}}[n] = \sum_{m=1}^{M} \exp\{j2\pi\left[f_0 + (m-1)f_p + \frac{1}{2}ut\right] t + j(m-1)\Delta\phi\}|_{t=nT_s} \tag{2}$$

$$s_{\mathrm{PC-MIMO}}[n] = \sum_{m=1}^{M}\sum_{i=1}^{I} \exp[j2\pi f_0 t + j\phi_m(i) + j(m-1)\Delta\phi] g(t - iT_1)|_{t=nT_s} \tag{3}$$

$$s_{\mathrm{FC-MIMO}}[n] = \sum_{m=1}^{M}\sum_{i=1}^{I} \exp\{j2\pi[f_0 + f_m(i)]t + j(m-1)\Delta\phi\} g(t - iT_1)|_{t=nT_s} \tag{4}$$

where exp() denotes the exponential function, M is the number of sub-carriers of MIMO radar signal, f_0 is the carrier frequency, $f_p = 1/T$ and $\triangle\phi$ denote the frequency interval and phase difference between adjacent sub-carriers, respectively, u denotes the chirp rate, I is the code length of coding signal, $T_s = 1/f_s$ is the sampling interval, f_s is the sampling rate, $\phi_m(i) \in \{0, \frac{2\pi}{L}, \ldots, (L-1)\cdot\frac{2\pi}{L}\}$ denotes the phase of sub-pulse i of the mth component, $f_m(i) \in \{0, \frac{1}{T_1}, \ldots, (I-1)\cdot\frac{1}{T_1}\}$ denotes the frequency of sub-pulse i of the mth component, L is the distinct phase number in PC-MIMO, T and T_1 represent the pulse and sub-pulse width, respectively, $g(t)$, $0 \le t \le T_1$ is the envelope function. Particularly, to ensure the orthogonality of components, $\varnothing_m(i)$ and $f_m(i)$ are usually obtained by intelligent algorithm, such as genetic algorithm and simulated annealing algorithm.

3. Recognition method

For the sake of convenience, S set is employed: S = {MP-MIMO, LFM-MIMO, PC-MIMO, FC-MIMO and SC signals}. This section will be divided into three parts. The first part classifies S set signals into three categories: SC signals S_0 = {SC signals}, non-coding MIMO radar signals S_1 = {MP-MIMO, LFM-MIMO} and coding MIMO radar signals S_2 = {PC-MIMO, FC-MIMO}. S_1 and S_2 set signals are recognized in second and third parts, respectively.

3.1 Instantaneous autocorrelation spectrum analyses

The signal pulse parameters can be extracted from instantaneous autocorrelation features. Since the frequency characteristics of different modulation types are diverse, instantaneous autocorrelation function can be utilized to the modulation recognition of MIMO radar signals. The instantaneous autocorrelation function is defined as

$$r[n, \Delta n] = s[n + \Delta n]s^*[n] \tag{5}$$

3.1.1. $S_1/(S_0,S_2)$ selection

(a) S_1 set signals analysis

The instantaneous autocorrelation of LFM-MIMO signal is

$$r_{\mathrm{LFM-MIMO}}[n, \Delta n] = \sum_{m=1}^{M}\sum_{l=1}^{M} \exp\left\{j2\pi \frac{f_0\Delta n + f_p[kn + (m-1)\Delta n]}{f_s} + j\pi u\frac{2n\Delta n + \Delta n^2}{f_s^2} + jk\Delta\phi\right\} \tag{6}$$

where $k = m - l$, $|k| \le M - 1$. If $k = 0$, it denotes the signal term. Otherwise, it denotes the cross terms.

For convenience, let $\Delta n = 1$, then we can get

$$r_{\mathrm{LFM-MIMO}}[n,1] = \sum_{m=1}^{M}\sum_{l=1}^{M} \exp\left[j2\pi\frac{f_0 + f_p(kn+m-1)}{f_s} + j\pi u\frac{2n+1}{f_s^2} + jk\Delta\phi\right] \tag{7}$$

Accordingly, the signal term is get as

$$\exp\left(j2\pi\frac{f_0}{f_s} + j\pi u\frac{2n+1}{f_s^2}\right)\sum_{m=1}^{M}\exp\left(j2\pi\frac{(m-1)f_p}{f_s}\right) \tag{8}$$

The cross term is obtained as

$$\exp\left(j2\pi\frac{f_0 + kf_p n}{f_s} + j\pi u\frac{2n+1}{f_s^2} + jk\Delta\phi\right)\sum_{m=|k|+1}^{M}\exp\left(j2\pi\frac{(m-1)f_p}{f_s}\right) \tag{9}$$

From the above, the moduli of signal term and cross term are $\left|\frac{\sin(M\pi f_p/f_s)}{\sin(\pi f_p/f_s)}\right|$ and $\left|\frac{\sin[(M-|k|)\pi f_p/f_s]}{\sin(\pi f_p/f_s)}\right|$, respectively. If $|k| = 1$, it is the biggest cross term.

Figure 1b shows the instantaneous autocorrelation spectrum of LFM-MIMO signal. The simulated MIMO radar has a ULA comprising four transmitting antennas with half-wavelength spacing between adjacent antennas. The simulated SNR is 5 dB. By the way, for the other parts of Figure 1, the simulation conditions are the same. For Figure 1b, the maximum peak results from signal term while other peaks are from cross terms. As we can see, the biggest cross term appears as the second peak in the autocorrelation spectrum. To extract signal features, we define the feature parameter: the ratio of second peak and maximum peak, which can be expressed as follows:

$$R_{\mathrm{Amplitute}} = \left|\frac{\sin[(M-1)\pi f_p/f_s]}{\sin(M\pi f_p/f_s)}\right| \tag{10}$$

If $u = 0$, Equation (7) is the instantaneous autocorrelation function of MP-MIMO. Since u is not related to (10), MP-MIMO and LFM-MIMO have the equivalent values of $R_{\mathrm{Amplitute}}$. Comparing Figure 1a with b, the fact is verified since the values of every peak are the same. Given the value ranges of parameters in Equation (10), the minimum value of $R_{\mathrm{Amplitute}}$ can be obtained.

In addition, by searching the peaks of instantaneous autocorrelation spectrum of non-coding MIMO radar signal, the number of sub-carriers can be obtained. For Figure 1, the simulated MIMO radar has four transmitting antennas. That is, the sub-carrier number is four. Seven peaks can be seen in Figure 1a,b. Six of them, resulted from cross terms in (9), are symmetrical. Together with the single frequency at center, the distinct frequency number is four. That is, the sub-carrier number is four for the received MIMO radar signal, which is equal to the actual sub-carrier number of non-coding MIMO radar signal. For the instantaneous autocorrelation spectrum of non-coding MIMO radar signal, supposing that the number of peaks is a, the sub-carrier number is $(a + 1)/2$.

Meanwhile, some signal modulation parameters of non-coding MIMO radar signal can be got from the instantaneous autocorrelation spectrum. For example, the chirp rate u and the frequency interval between adjacent sub-carriers f_p. They can be estimated from the location of peaks.

(b)S_2 set signals analysis

For PC-MIMO and FC-MIMO, substituting Equations (3) and (4) into Equation (5), respectively, the instantaneous autocorrelation functions are as follows:

$$r_{\mathrm{PC-MIMO}}[n,1] = \exp\left(j2\pi\frac{f_0}{f_s}\right)\sum_{m=1}^{M}\sum_{l=1}^{M}\exp\left\{j\left[\phi_m^{n+1} - \phi_l^n + (m-l)\Delta\phi\right]\right\} \tag{11}$$

$$r_{\mathrm{FC-MIMO}}[n,1] = \exp\left(j2\pi\frac{f_0}{f_s}\right)\sum_{m=1}^{M}\sum_{l=1}^{M}\exp\left[j2\pi\frac{\left(f_m^{n+1} - f_l^n\right)n + f_m^{n+1}}{f_s} + j(m-l)\Delta\phi\right] \tag{12}$$

where the superscript of $\varnothing$ and f denote the location of the code.

For Equation (11), since $\phi_m^{n+1} - \phi_l^n = \mathrm{const}$ in a sub-pulse, $r_{\mathrm{PC\text{-}MIMO}}[n,1]$ is constant in a sub-pulse. If n is the last sampling points of a sub-pulse, then $n + 1$ is in the next sub-pulse. So, the value of $\left(\phi_m^{n+1} - \phi_l^n\right)$ suddenly changes and mutations appear in sub-pulses junctions. The constant values result in zero frequency. The mutations will bring about some low frequencies, the amplitudes of which are very small compared with the zero frequency. That is, only one obvious peak appears at the zero frequency in the frequency spectrum of PC-MIMO.

For Equation (12), there are $M \times M$ components in a sub-pulse. M components, which are from $f_m^{n+1} - f_l^n = 0$ in the case of $m = 1$ in a sub-pulse, result in zero frequency. If $m \neq l$, then $f_m^{n+1} - f_l^n = \Delta f$ in a sub-pulse. There will be $M^2 - M$ cross terms, which result in low

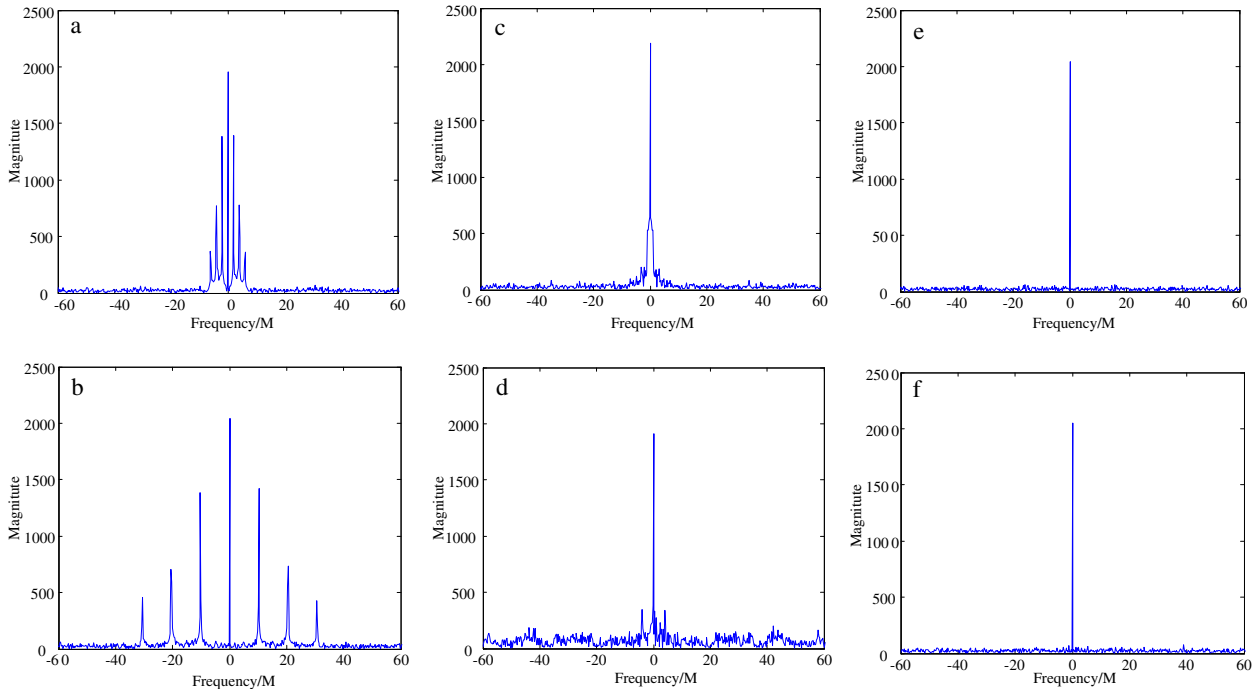

Figure 1 Instantaneous autocorrelation spectrum of S set signals: (a) MP-MIMO, (b) LFM-MIMO, (c) PC-MIMO, (d) FC-MIMO, (e) MP, (f) PC.

frequencies. Considering the symmetry, there are $(M^2-M)/2$ positive frequency components. $M-1$ components have the same frequency in the worst case. However, since the code length I is far greater than the number of sub-carrier M generally, the codes of each component are different in the same sub-pulse. So, the values of $\left(f_m^{n+1}-f_l^n\right)$ in a sub-pulse are diverse. The other sub-pulses as well. That is, the energies of the cross terms almost cannot be superimposed. Only one obvious peak appears at the zero frequency in the frequency spectrum of FC-MIMO.

The instantaneous autocorrelation spectrums of PC-MIMO and FC-MIMO signals are shown in Figure 1c,d, respectively. As can be seen, most of the energies gather at the zero frequency while some appear at low frequencies for both PC-MIMO and FC-MIMO, which verify the above analysis. As a result, values of $R_{\text{Amplitute}}$ for coding MIMO radar signals are very small, which are less than the value of non-coding MIMO signals. The same to the SC signals, which can be seen in Figure 1e,f.

Consequently, taking the ratio of second peak and maximum peak as the feature parameter, S_1 signals are discriminated from S_0 and S_2 set, which is expressed as follows:

$$\begin{cases} R_{\text{Amplitute}} \geq \gamma \Rightarrow S_1 \\ R_{\text{Amplitute}} < \gamma \Rightarrow S_0/S_2 \end{cases} \tag{13}$$

where γ is the value of the threshold.

Assuming that $4 \leq M \leq 50$, $0.005 \leq f_p/fs \leq 0.02$, which satisfy most of the signal environment, the minimum value of Equation (10) is 0.7502. That is, for non-coding MIMO radar signal, the value of R is always greater than 0.7502. Obviously, for S_0 or S_2 set signals, the value of R is smaller than 0.7502. As a consequence, 0.75, the value of the threshold, permits classifying between S_1 set and other modulation types.

3.1.2. S_0/S_2 selection

Let $\Delta n = 0$, then $r[n,0] = s[n]s^*[n]$.

For SC signals, $r_{\text{SC}}[n,0] = 1$. As a result, the frequency of $r_{\text{SC}}[n,0]$ is zero.

For coding MIMO radar signals, according to (3) and (4), we can get the $r[n,0]$ of PC-MIMO and FC-MIMO signals, which can be expressed as follows:

$$r_{\text{PC-MIMO}}[n,0] = \sum_{m=1}^{M}\sum_{l=1}^{M} e^{j[\phi_m(n)-\phi_l(n)]} \tag{14}$$

$$r_{\text{FC-MIMO}}[n,0] = \sum_{m=1}^{M}\sum_{l=1}^{M} e^{j2\pi[f_m(n)-f_l(n)]} \tag{15}$$

From Equations (14) and (15), we can see that there are some mutations in the correlation function. As a result, they will bring about some low-frequency components. Since the frequency of $r_{SC}[n,0]$ is zero, this allows us to discriminate SC signals from coding MIMO radar signals.

Employing Fourier transform on the $r[n,0]$, which is obtained from S_0 and S_2 set signals, we can obtain its positive frequency spectrum.

$$R_{r[n,0]}[k] = |\mathrm{DFT}(r[n,0])|, \quad k = 1, 2, \ldots, N_{\mathrm{DFT}}/2 \tag{16}$$

where N_{DFT} denotes the points of discrete Fourier transform (DFT). Then we divide the positive frequency into two segments. One is the low-frequency segment; the other is the rest part.

$$\begin{cases} R1_{r[n,0]}[k], & k = 1, 2, \ldots, N1 \\ R2_{r[n,0]}[k], & k = N1+1, N1+2, \ldots, N_{\mathrm{DFT}}/2 \end{cases} \tag{17}$$

After that, we define the feature parameter R_{mean} as

$$R_{\mathrm{mean}} = \frac{\mathrm{Mean}\left(R1_{r[n,0]}\right)}{\mathrm{Mean}\left(R2_{r[n,0]}\right)} \tag{18}$$

where Mean() is the mean function. Since $r_{\mathrm{SC}}[n,0] = 1$ for SC signals, the frequency of $r_{SC}[n,0]$ is zero, which implies that $R1_{r[n,0]}$ and $R2_{r[n,0]}$ are only affected by noise. Thus, R_{mean} approximately equals 1 in the additive white Gaussian noise (AWGN) condition. For coding MIMO radar signals, according to Equations (14) and (15), there are a few mutations in the $r[n,0]$. Hence, they will lead to some low-frequency components, the values of ratio R_{mean} of coding MIMO radar signals are always greater than 1. This permits us to discriminate SC signals from coding MIMO radar signals.

Consequently, setting proper thresholds ς, S_2 set signals are discriminated from S_0 set signals, which is expressed as follows:

$$\begin{cases} R_{\mathrm{mean}} \geq \varsigma \Rightarrow S_2 \\ R_{\mathrm{mean}} < \varsigma \Rightarrow S_0 \end{cases} \tag{19}$$

MP-MIMO/LFM-MIMO selection

According to the first part, S set signals are divided into three categories. To recognize the modulation type of MIMO radar signal, we need to keep working on S_1 set and S_2 set signals. In this part, our attention is focused on the S_1 set. The goal is to discriminate MP-MIMO signal from LFM-MIMO signal.

Selecting two different lengths of time window for the signal and employing DFT on them, we can get

$$\begin{cases} S_a[k] = |\mathrm{DFT}(s_a[n])|, & s_a[n] = s[n], n = 1, 2, \ldots N2 \\ S_b[k] = |\mathrm{DFT}(s_b[n])|, & s_b[n] = s[n], n = 1, 2, \ldots N, N > 2N2 \end{cases} \tag{20}$$

As can be seen in (20), s_a is contained in s_b and the sampling length of s_b is greater than s_a.

If the maximum value of S_a is noted by Max(S_a), and the corresponding frequency number is $k_{\max}$, then the value of $S_b[k_{\max}]$ is obtained. We define the following feature parameter

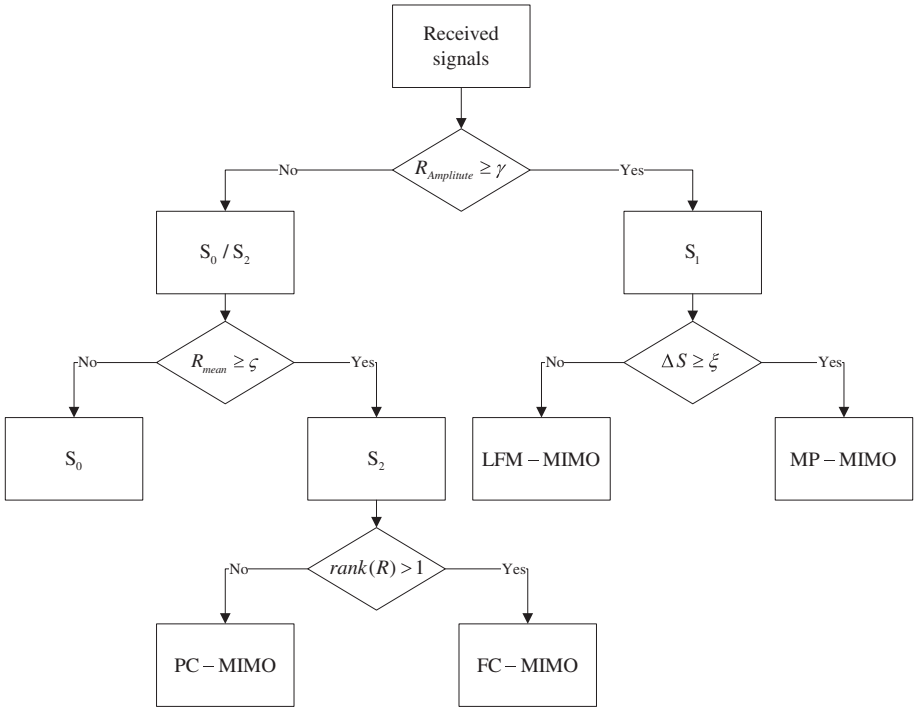

Figure 2 Functional flowchart for the proposed recognition method.

Table 1 Simulation parameters

Simulation parameters	f_0 (MHz)	f_s (GHz)	T (μs)	u (THz/s)	T_{1PC} (μs)	T_{1FC} (μs)	L
Condition 1	100	0.5	5	2	0.25	0.25	4
Condition 2	100	2	5	4	0.05	0.1	6

L is the distinct phase number of PC/PC-MIMO, T_{1PC} and T_{1FC} are the sub-pulse width of PC/PC-MIMO and FC/FC-MIMO, respectively. The simulation results are based on 1000 Monte Carlo trials for each modulation type and each SNR value. Particularly, we consider that SC signals are correctly recognized when the simulation results are S_0 set signal but not the exact modulation type.

$$\Delta S = \mathrm{Max}(S_a) - S_b[k_{\max}] \tag{21}$$

The frequency of MP-MIMO signal is not affected by the time while LFM-MIMO signal is modulated along time. That is, for MP-MIMO signal, the energy at a frequency is increasing with the increase of sampling points while the LFM-MIMO is not, for the energy present at the extra frequencies. Setting a proper threshold ξ, MP-MIMO signal and LFM-MIMO signal are separated.

$$\begin{cases} \Delta S \geq \xi \Rightarrow \mathrm{MP-MIMO} \\ \Delta S < \xi \Rightarrow \mathrm{LFM-MIMO} \end{cases} \tag{22}$$

3.3. PC-MIMO/FC-MIMO selection

The SNEA is employed to recognize the signals of S_2 set in this part. For the sake of convenience, only the first code length signal is chosen. That is, the signal section going to be analyzed is $s(n), n < T_1/T_s$. We first construct the observation matrix

$$S_{ab} = \begin{bmatrix} s[1] & s[2] & \dots & s[N] \\ s[2] & s[3] & \dots & s[N+1] \\ \vdots & \vdots & \ddots & \vdots \\ s[Mr] & s[1+Mr] & \dots & s[N-1+Mr] \end{bmatrix} \in C^{M_r \times N} \tag{23}$$

and then get its autocorrelation matrix

$$R = \frac{1}{N} S_{ab} S_{ab}^H = \begin{bmatrix} r[0] & r[-1] & \dots & r[-Mr+1] \\ r[1] & r[0] & \dots & r[-Mr+2] \\ \vdots & \vdots & \ddots & \vdots \\ r[Mr-1] & r[Mr-2] & \dots & r[0] \end{bmatrix} \in C^{Mr \times Mr} \tag{24}$$

where $N - 1 + M_r < T_1/T_s$.

For PC-MIMO signal, according to Equation (3), we have

$$s_m[n+k] = \exp(j2\pi f_0 k) s_m[n] \tag{25}$$

To simplify expressions, $T_s = 1$ is employed in the calculation.

Let

$$A_0 = \begin{bmatrix} 1 & 1 & \cdots & 1 \\ e^{j2\pi f_0 1} & e^{j2\pi f_0 1} & \dots & e^{j2\pi f_0 1} \\ \vdots & \vdots & \cdots & \vdots \\ e^{j2\pi f_0 (M_r-1)} & e^{j2\pi f_0 (M_r-1)} & \dots & e^{j2\pi f_0 (M_r-1)} \end{bmatrix} \in C^{M_r \times M} \tag{26}$$

$$S_0 = \begin{bmatrix} s_1[1] & s_1[2] & \cdots & s_1[N] \\ s_2[1] & s_2[2] & \cdots & s_2[N] \\ \vdots & \vdots & \cdots & \vdots \\ s_M[1] & s_M[2] & \cdots & s_M[N] \end{bmatrix} \in C^{M \times N} \tag{27}$$

Obviously, rank(A_0) = 1, where rank(*) denotes the rank of matrix *. Observing Equation (23), we have $S_{ob} = A_0 S_0$. Then $R = A_0 S_0 S_0^H A_0^H / N$. According to the nature of rank, it is easy to get that rank(R) = 1 for PC-MIMO signal.

Table 2 Confusion matrices for Ω_1

Input modulation type	Classifier output					
	Condition 1 (Ω_1)			Condition 2 (Ω_1)		
	S_0	S_1	S_2	S_0	S_1	S_2
MP	999	0	1	1000	0	0
LFM	999	0	1	1000	0	0
MP-MIMO(4)	0	1000	0	0	1000	0
LFM-MIMO(4)	0	1000	0	0	1000	0
PC-MIMO(4)	2	0	998	0	0	1000
FC-MIMO(4)	0	0	1 000	10	0	990

Table 3 Confusion matrices for Ω_2

Input modulation type	Classifier output					
	Condition 1 (Ω_2)			Condition 2 (Ω_2)		
	S_0	S_1	S_2	S_0	S_1	S_2
PC	1000	0	0	1000	0	0
FC	999	0	1	1000	0	0
MP-MIMO(4)	0	1000	0	0	1000	0
LFM-MIMO(8)	0	1000	0	0	1000	0
PC-MIMO(10)	8	0	992	0	1	999
FC-MIMO(12)	0	0	1000	0	0	1000

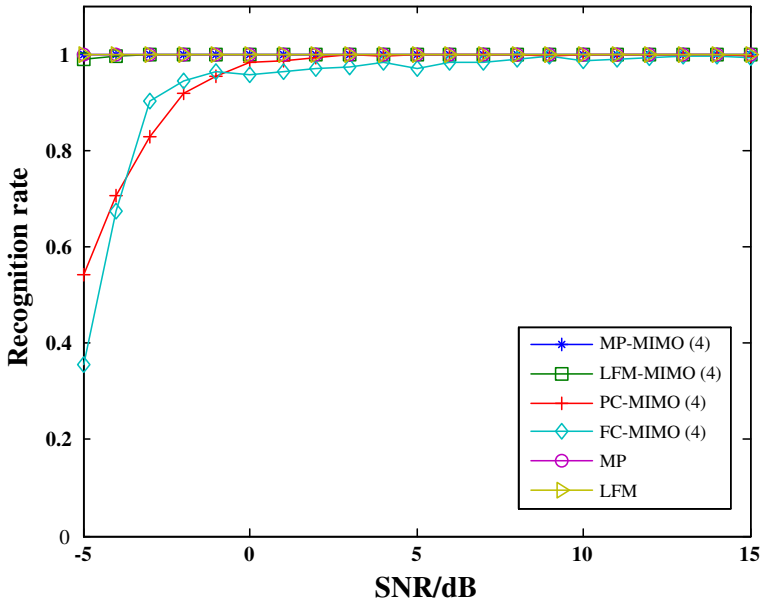

Figure 3 The recognition rate versus SNR (on the condition of 1 for Ω_1).

For FC-MIMO signal, according to (4), we have

$$s_m[n+k] = \exp\{j2\pi[f_0 + f_m(n)]k\}s_m[n] \tag{28}$$

Let

$$A_1 = \begin{bmatrix} 1 & 1 & \cdots & 1 \\ e^{j2\pi(f_0+f_1)1} & e^{j2\pi(f_0+f_2)1} & \cdots & e^{j2\pi(f_0+f_M)1} \\ \vdots & \vdots & \cdots & \vdots \\ e^{j2\pi(f_0+f_1)(M_r-1)} & e^{j2\pi(f_0+f_2)(M_r-1)} & \cdots & e^{j2\pi(f_0+f_M)(M_r-1)} \end{bmatrix} \in C^{M_r \times M} \tag{29}$$

$$S_0 = \begin{bmatrix} s_1[1] & s_1[2] & \cdots & s_1[N] \\ s_2[1] & s_2[2] & \cdots & s_2[N] \\ \vdots & \vdots & \cdots & \vdots \\ s_M[1] & s_M[2] & \cdots & s_M[N] \end{bmatrix} \in C^{M \times N} \tag{30}$$

where $f_1, f_2, \ldots, f_M$ denote the first frequency code of each component. To ensure the orthogonality between components, the values of $f_1, f_2, \ldots, f_M$ are not equal. According to Equations (29) and (30), we have $S_{ob} = A_1 S_0$

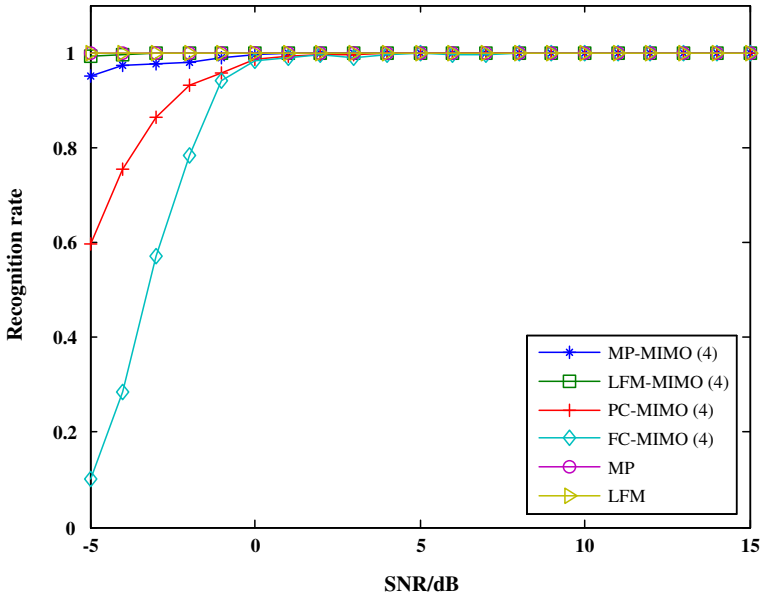

Figure 4 The recognition rate versus SNR (on the condition of 2 for Ω_1).

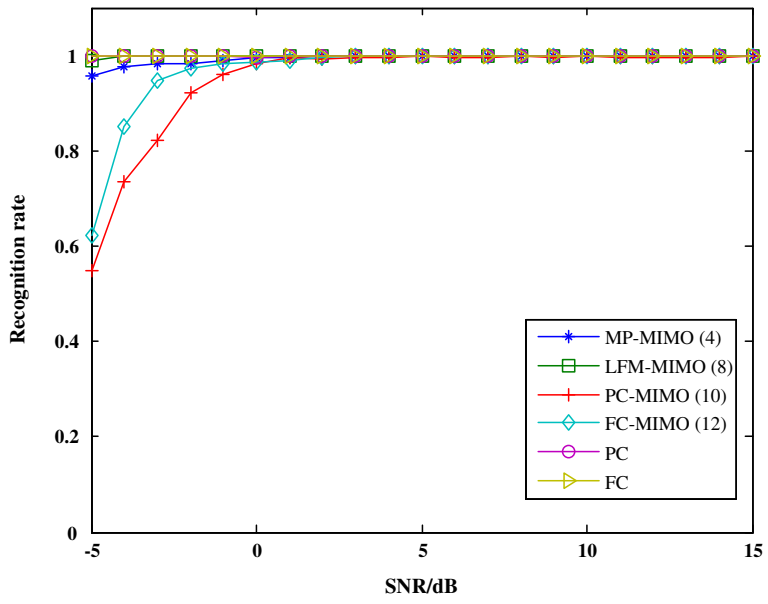

Figure 5 The recognition rate versus SNR (on the condition of 1 for Ω_2).

and $R = A_1 S_0 S_0^H A_1^H / N$ for FC-MIMO signal. Substituting Equation (4) into S_0, we can obtain that rank(S_0) = M. If $M_r > M$, then rank(A_0) = M, and so rank(R) = M for FC-MIMO signal. Hence, PC-MIMO signal and FC-MIMO signal are recognized. Meanwhile, the number of sub-carriers of FC-MIMO signal is obtained by the rank of R.

Here, Akaike Information Criterion [13] is adopted to calculate the rank of the autocorrelation matrix. By comparing the rank of autocorrelation matrix with 1, PC-MIMO and FC-MIMO are discriminated. That is

$$\begin{cases} rank(R) = 1 \Rightarrow \text{PC} - \text{MIMO} \\ rank(R) > 1 \Rightarrow \text{FC} - \text{MIMO} \end{cases} \tag{31}$$

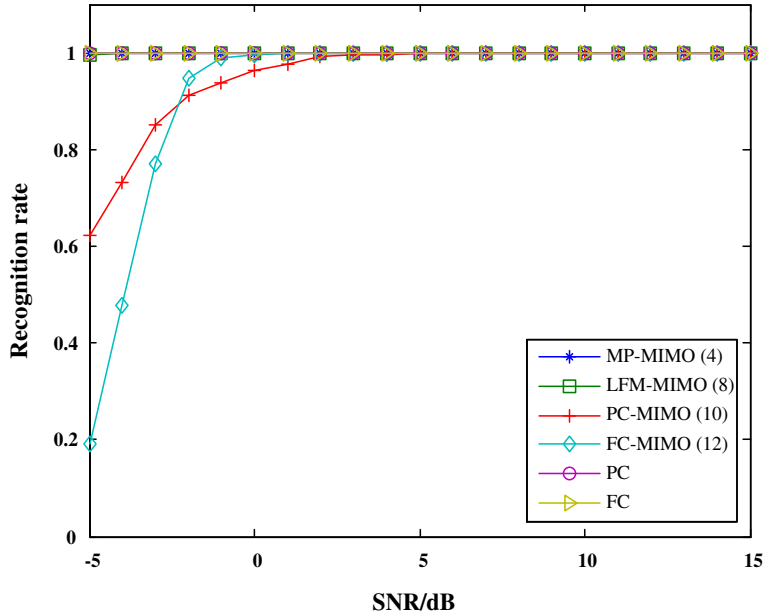

Figure 6 The recognition rate versus SNR (on the condition of 2 for Ω_2).

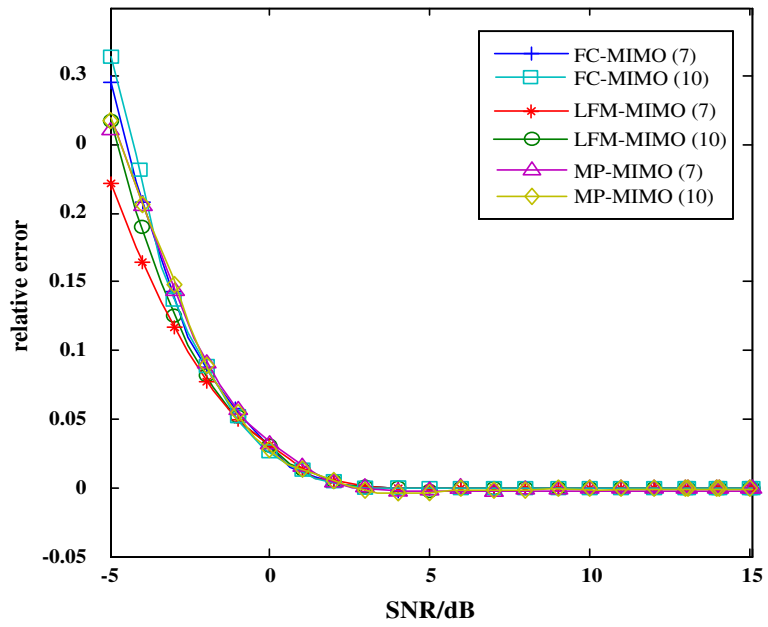

Figure 7 The relative error of estimated sub-carrier numbers of Ω_3.

At last, the modulation recognition method can be summarized as following flowchart in Figure 2.

4. Simulation and analysis

Simulation results are shown in this section. Modulation types in S set, which are given by Ω_1 and Ω_2, are used to test the validity of the proposed approach.

$$\Omega_1 = \left\{ \begin{array}{l} \mathrm{MP}, LFM, \\ \mathrm{MP} - MIMO(4), LFM - MIMO(4), \\ PC - MIMO(4), FC - MIMO(4) \end{array} \right\}$$

$$\Omega_2 = \left\{ \begin{array}{l} \mathrm{PC}, FC, \\ \mathrm{MP} - MIMO(4), LFM - MIMO(8), \\ PC - MIMO(10), FC - MIMO(12) \end{array} \right\}$$

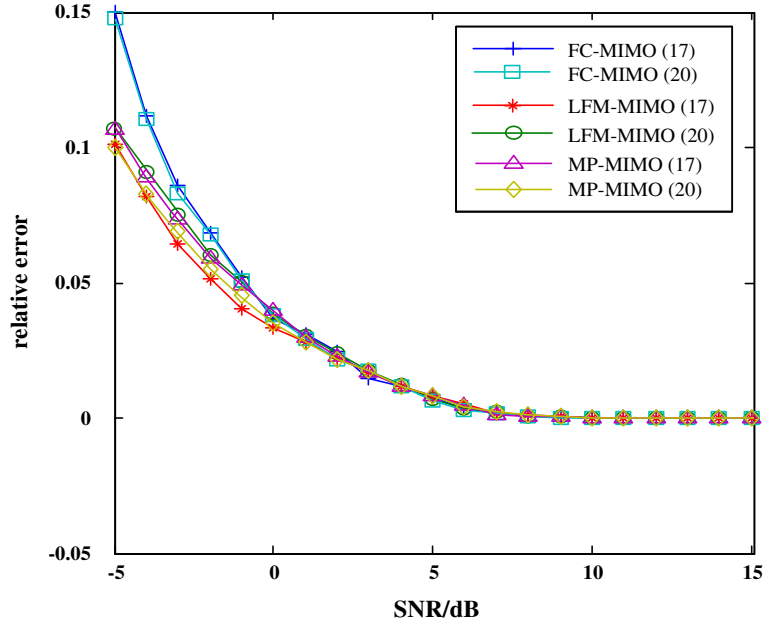

Figure 8 The relative error of estimated sub-carrier numbers of Ω_4.

The figure following each MIMO radar signal denotes the number of sub-carriers. Suppose that the received signals are imbedded in complex AWGN and are rectangular pulse shape. Particularly, experiments are operated on two different simulation conditions, which are showed in Table 1.

4.1. The classification results

First, we study the performance of the proposed classifier with several values of SNR. Because of lack of space, simulation results under 0 dB is selected as representatives. Confusion matrices for Ω_1 and Ω_2 are shown in Tables 2 and 3, respectively, on two different conditions listed in Table 1. 1000 signals are utilized for each modulation scheme.

From Tables 2 and 3, we can see that the approach based on instantaneous autocorrelation spectrum successfully classifies the S set signals into three categories. The correct classify rates are all over 90%. It shows that this approach is well prepared for the following modulation recognition. Moreover, the performance shown in Tables 2 and 3 is alike on the constant condition, which indicates that the method is unaffected by sub-carrier numbers of MIMO radar signal.

4.2. The recognition results

Figures 3, 4, 5, and 6 represent the final recognition results. As can be seen, the total recognition probability is over 90% when the value of SNR is as low as 0 dB. The results demonstrate that the modulation types are well recognized by the suggested method.

This method presents an excellent performance for non-coding MIMO radar signals, which is of high recognition rate even if the value of SNR is −5 dB. Comparing Figure 3 with Figure 5, the recognition performance is almost the same, which demonstrates that the sub-carrier number influences the proposed method slightly. This can also be illustrated by comparing Figure 4 with Figure 6. Comparing Figure 4 with Figure 3, the performance of FC-MIMO signal in low SNR slightly decreased, which results from high code rate. The same conclusion can be obtained by comparing Figure 5 with Figure 6.

4.3. The estimation results

As is mentioned above, some parameters of MIMO radar signal can be estimated simultaneously by the recognition method. Here, the estimation results of sub-carrier numbers of non-coding MIMO radar signal and FC-MIMO radar signal are presented as representative.

The simulation is conducted on the condition 1. The signals used to test are Ω_3 and Ω_4, which can be expressed as

$$\Omega_3 = \left\{ \begin{array}{l} \mathrm{FC}-\mathrm{MIMO}(7), \mathrm{FC}-\mathrm{MIMO}(10), \\ \mathrm{LFM}-\mathrm{MIMO}(7), \mathrm{LFM}-\mathrm{MIMO}(10), \\ \mathrm{MP}-\mathit{MIMO}(7), \mathit{LFM}-\mathit{MIMO}(10) \end{array} \right\},$$

$$\Omega_4 = \left\{ \begin{array}{l} \mathrm{FC}-\mathrm{MIMO}(17), \mathrm{FC}-\mathrm{MIMO}(20), \\ \mathrm{LFM}-\mathrm{MIMO}(17), \mathrm{LFM}-\mathrm{MIMO}(20), \\ \mathrm{MP}-\mathit{MIMO}(17), \mathit{LFM}-\mathit{MIMO}(20) \end{array} \right\}.$$

Figures 7 and 8 show the relative error of estimation. As can be seen, the sub-carrier numbers of MIMO radar signal are almost correctly estimated when the value of SNR above 0 dB. If the values of SNR below 0 dB, the relative error of estimation is acceptable. Comparing Figure 7 with Figure 8, the relative error of Figure 8 is smaller than Figure 7. This results from the calculation methods of relative error. By the proposed approach, for the different sub-carriers, the absolute error changes slightly. Then the relative error decreases with the increases of sub-carriers.

5. Conclusions

This article presents an approach to recognize the modulation type of MIMO radar signals for the first time. Three feature parameters are proposed in the recognition method. First, the intercepted signal is classified based on the instantaneous autocorrelation spectrum. Then, taking advantage of the difference in frequency domain, MP-MIMO signal and LFM-MIMO signal are discriminated. At last, SNEA is employed to recognize PC-MIMO signal from FC-MIMO signal. Besides, sub-carrier numbers of non-coding MIMO radar signal and FC-MIMO signal are estimated simultaneously. Simulation results verify that the proposed method can extract the features of each modulation type, and effectively recognize the signals in the given set. This result can be provided as an analysis reference for the research of MIMO radar countermeasures.

Competing interests
The authors declare that they have no competing interests.

Received: 11 December 2012 Accepted: 1 February 2013
Published: 14 March 2013

References

1. J Li, P Stoica, *MIMO Radar Signal Processing* (Wiley, New Jersey, 2008)
2. DW Bliss, KW Forsythe, Multiple-input multiple-output (MIMO) radar and imaging: degrees of freedom and resolution, in *Proceedings of the Thirty-Seventh Asilomar Conference on Signals, Systems and Computers, vol. 1* (, California, USA, 2003), pp. 54–59. November
3. KW Forsythe, DW Bliss, GS Fawcett, *Multiple-input multiple-output (MIMO) radar: performance issues, in Proceedings of the Thirty-Eighth Asilomar Conference on Signals, Systems and Computers*, vol. 1 (USA, California, November 2004). pp. 310–315
4. J Li, P Stoica, LZ Xu, W Roberts, On parameter identifiability of MIMO radar. IEEE Signal Process. Lett. **14**(12), 968–971 (2007)
5. B-C Liang, Electronic reconnaissance technology for MIMO radar. Shipboard Electron. CM (in Chinese) **31**(5), 17–19 (2008)

6. R-Y Xing, C-G Zhou, T-J Tong, The characteristic of foreign MIMO radar system and the space electronic reconnaissance and countermeasure. Foreign Inf. War (in Chinese) **1**, 38–39 (2007)
7. X-W Tang, J Tang, B Tang, A new electronic reconnaissance technology for MIMO radar, in *Proceedings of the 2011 IEEE CIE International Conference on Radar, vol. 1* (, Chengdu, China, 2011), pp. 79–83. October
8. J Chen, Y-H Kuo, X-L Liu, Modulation identification for MIMO-OFDM signals, in *Proceedings of the IET Conference on Wireless, Mobile and Sensor Networks, vol. 1* (, Shanghai, China, 2007), pp. 1013–1016. December
9. K Hassan, W Hamouda, I Dayoub, Blind modulation identification for MIMO systems, in *Proceedings of the IEEE Global Telecommunications Conference, vol. 1* (, Miami, USA, 2010), pp. 1–5. December
10. B Liu, Z-S He, J-K Zeng, B-Y Liu, Polyphase Orthogonal Code Design for MIMO Radar Systems, in *Proceedings of the CIE International Conference on Radar, vol. 1* (, Shanghai, China, 2006), pp. 1–4. October
11. B Liu, Z-S He, Orthogonal discrete frequency-coding waveform design for MIMO radar. Chin. J. Electron. **25**(4), 471–476 (2008)
12. B Liu, *Research on generation of orthogonal waveform and signal processing for MIMO radar. Dissertation, University of Electronic Science and Technology (in Chinese)*, 2008
13. M Wax, T Kailath, Detection of signals by information theoretic criteria. IEEE Trans. Acoust. Speech Signal Process. **33**(2), 387–392 (1985)

doi:10.1186/1687-1499-2013-66
Cite this article as: Wang *et al.*: **An approach to the modulation recognition of MIMO radar signals.** *EURASIP Journal on Wireless Communications and Networking* 2013 **2013**:66.